The Statistical Characteristics of One- and Two-Layer Cloudiness Based on Laser Sounding Data

V. V. Zuev, V. D. Burlakov, and A. V. El'nikov
Institute of Atmospheric Optics
Tomsk, Russia

Introduction

Earlier lidar observations of the middle- and high-level clouds, conducted as part of the Atmospheric Radiation Measurement (ARM) Program, frequently revealed a significant relationship between the cloud layers, including those located at different atmospheric levels. At the same time, current models of solar radiative transfer in two-layer clouds a priori assume a statistical independence of cloud layers; so of primary concern here was to study possible causes for such a relationship and potential conditions for its breakdown.

Studies were performed at the Siberian lidar station of the Institute of Atmospheric Optics, and the instrumentation included a lidar system with two laser transmitters and two receiving apertures. Lidar observations during night conditions, with minimum skylight background, were taken using a high-frequency (2.5-kHz) Cu-vapor laser with a mean power of 2 W at a wavelength of 510 nm and a large receiving mirror 2.2 m in diameter. In daytime measurements, contaminated by bright skylight background, we used a low-frequency (10-Hz) Nd:YAG solid laser, having 150 mJ energy per pulse at a wavelength of 1064 nm, as well as a receiving mirror 0.3 m in diameter. In both cases, lidar returns were recorded in the photon counting regime. The parameters of the lidar system ensured a high level of accumulating signals from middle- and high-level clouds for 1 s (at night) and 3-5 s (during the day). On the other hand, the level of lidar return signals, accumulated within these time intervals, particularly during the day, is too low to perform a calibration of the lidar signal on the segment of sensing path outside the clouds and, thus, to correctly calculate the extinction coefficient and associated cloud optical depth τ_{cl}. For this reason, in the present work, we utilized statistics of the function

$$\varphi(t) = \sum_{H_D}^{H_U} F(H,t) =$$

$$= \sum_{H_D}^{H_U} N(H) \cdot H^2 / \beta(H) / F(H_{NORM})$$

where H is the height; N(H) is the number of photons returning from the sensing path; $\beta(H)$ is the model molecular scattering coefficient; $F(H_{NORM})$ is the value of the function F at calibration altitude H_{NORM}; H_U and H_D are the cloud top and bottom heights. This function is closely related to τ_{cl} (with a

correlation coefficient of 0.9-0.93). Also, the representation of the cloud optical depth in terms of the function F(H) substantially simplifies the task of determining cloud top and bottom heights because in the clear atmosphere the F(H) value is close to one.

The auto- and cross-correlation functions $K_A(L)$ and $K_C(L)$ are used in the analysis of statistical characteristics of time variations of the random functions. The expression for the cross-correlation function has the form

$$K_C(L) = \frac{1}{(Z-1)\cdot\sqrt{D_\varphi}\cdot\sqrt{D_\phi}}\sum_{i=1}^{Z}(\varphi_i - \bar{\varphi})\cdot(\phi_i - \bar{\phi})$$

where φ_i and ϕ_i are the values of the functions $\varphi(t)$ and $\phi(t)$ at a fixed time t; Z is the number of counts; D_φ and D_ϕ are the variances of the functions φ and ϕ; $\bar{\varphi}$ and $\bar{\phi}$ are the third-order polynomials of the functions $\varphi(t)$ and $\phi(t)$ that remove from realizations the mean and slowly varying trend; and L is the time lag between studied realizations. $K_C(L)$ was calculated in both directions relative to zero. The autocorrelation function is calculated from this same formula, when $\varphi(t) = \phi(t)$, but in the direction of positive L values. The auto- and cross-correlation analysis can reliably reveal the weakening of relationships in the studied time series. For instance, when $\varphi(t)$ is formed randomly, $K_A(L)$ resembles a δ-function.

Figure 1 presents a time series of the function φ together with autocorrelation functions calculated for the corresponding time intervals (indicated in the figure). Measurements at 510 nm are made in one-layer cirrus clouds at nighttime on August 13, 1998, with counts sampled every 1.2 s. As seen from the figure, the time series of the function φ contain variations with quite regular structure. The time scales of these variations range from 20 s up to 20 min. For the 20-min long period, the function φ (i.e., the optical depth) completes the entire cycle of its variation, from the lowest (near-zero) to highest and, backward, to lowest values. The structure of the variations changes from one time period to another, and so do statistical characteristics, even within a single cloud. In the figure, there is a time segment with essentially non-stationary behavior of the function φ; within it, the autocorrelation function calculated from the time series of the function φ, closely resembles a δ-function (segment B). On segments A and C, the time variations of the function φ differ, but their autocorrelation functions are

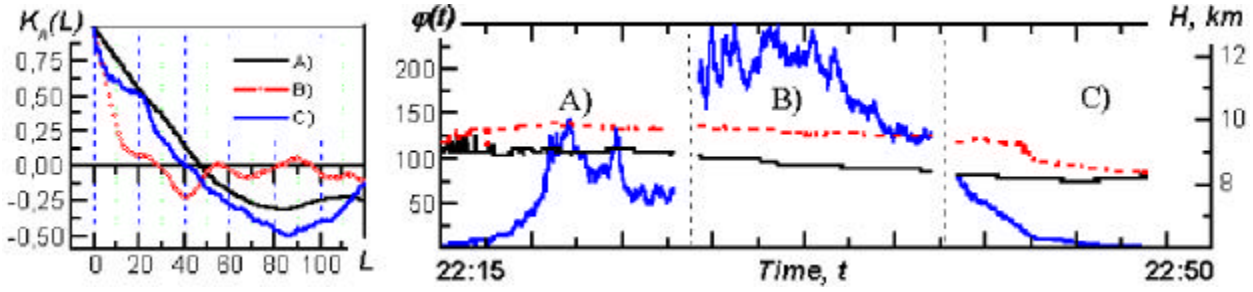

Figure 1. Temporal behavior of the height of the upper (dash line) and lower (thin solid line) boundaries, function $\varphi(t)$ (thick solid line) of the cirrus cloud, and $K_A(L)$ of the function φ for the corresponding intervals.

close in shape; their smoother decline, than the $K_A(L)$ decrease on segment B, with growing lag L suggests a closer relationship on these segments. We will characterize the size of temporal cloud inhomogeneities by the temporal correlation radius defined as a time required for autocorrelation function to reach 0.5; in these terms, the temporal correlation radius will be 30 s on segments A and C and 14 s on segment B.

More regular periodic variations of cloud characteristics are shown in Figure 2, which presents a time series of daylight lidar measurements in two-layer clouds at a wavelength 1064 nm. The counts were sampled every 6.4 s. As in Figure 1, plotted are time series of cloud top and bottom heights, behaviors of the functions φ(t), and their $K_A(L)$, but now for both cloud layers; also shown is the cross-correlation function $K_C(L)$ of time series φ(t) of the upper and lower layers (shown in the dashed line in the $K_C(L)$ plot are the confidence limits). In Figure 2, we clearly see well defined, asynchronous wave structures with periods of 570 s in both cloud layers. Also of note is that the time behavior of the function f of the cloud top height is in phase with that of the cloud bottom height. A well defined periodicity (580 s) in time series of φ(t) of both layers translates into very similar behavior of autocorrelation functions; and also it is reflected in the behavior of cross-correlation function $K_C(L)$, thus causing a close correlation between the layers.

Figure 3 is the same as Figure 2, but for parameters and characteristics obtained on the same day from some other (two hours later) series of lidar measurements. It is seen that, for the lower cloud layer, the variations of the function f are random in character ($K_A[L]$ looks like δ-function). However, the upper cloud layer preserves periodic properties. Values of cross-correlation function suggest that the cloud layers are practically uncorrelated.

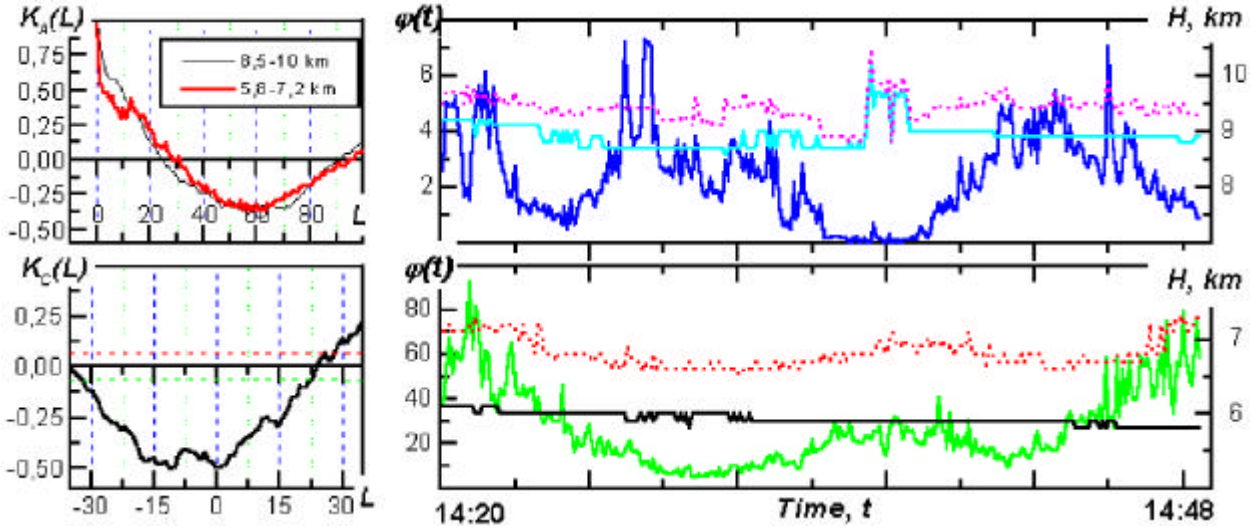

Figure 2. Temporal behavior (14:20-14:48) of the height of the upper (dash line) and lower (thin solid line) boundaries, function φ(t) (thick solid line) of the two-layer cloudiness, and $K_A(L)$, $K_C(L)$ of function φ for the corresponding cloud layers.

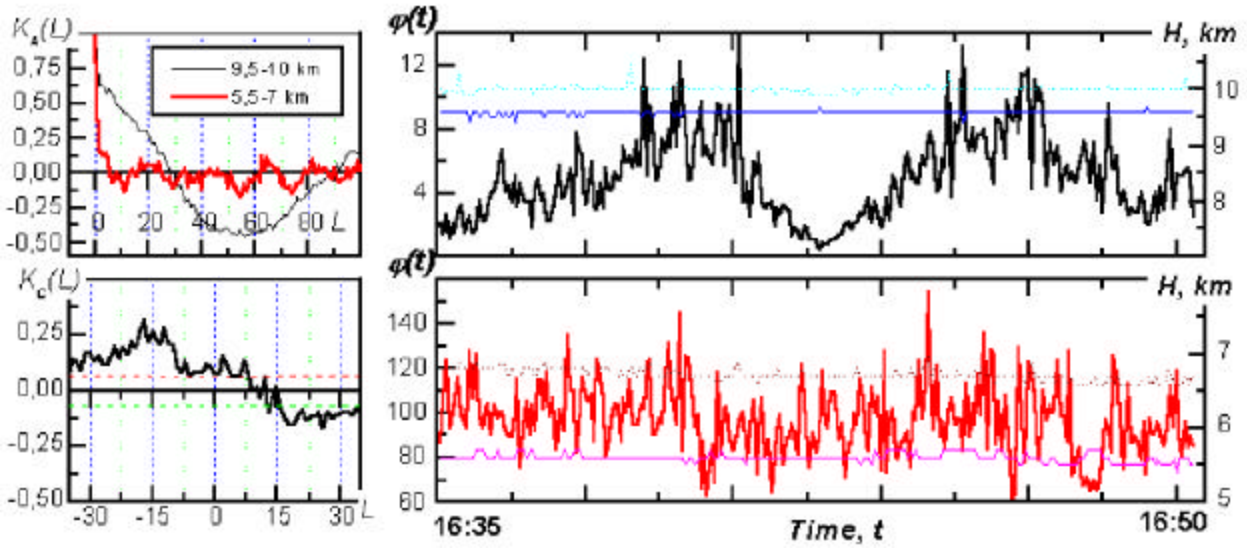

Figure 3. Temporal behavior (16:35-16:50) of the height of the upper (dash line) and lower (thin solid line) boundaries, function φ(t) (thick solid line) of the two-layer cloudiness, and $K_A(L)$, $K_C(L)$ of function φ for the corresponding cloud layers.

These wavy structures, with periods from 20 to 630 s, are most likely due to the internal gravity waves, which in turn may be caused, in particular, by the atmospheric jet streams. These waves generate an overall wavy pattern and associated periodicity of atmospheric thermodynamic parameters, thereby giving rise to the relationship between different cloud layers, on the basis of common cloud-formation processes.

The results of lidar studies suggest that the observed relationship between cloud layers may result from modulation of independent cloud layers by internal gravity waves. Neglect of this relationship may lead to incorrect interpretation of radiation measurements made with different temporal and spatial resolutions. This is especially true for lidar measurements, since lidars inherently possess a high speed of operation and narrow fields of view (FOVs). To make the lidar and wide-FOV radiometer measurements compatible, it is necessary to average the lidar data over a full period of a dominating internal gravity wave. Moreover, this time averaging of lidar data additionally increases the accuracy of determining cloud boundary heights and cloud optical depth.

This work was supported by the U.S. Department of Energy's (DOE) ARM Program under contract No. 35654-A-Q1.

Bibliography

Gossard, E. E., and W. H. Hooke, 1975: Waves in the Atmosphere, Elsevier Scientific Publishing Company, Amsterdam-Oxford-New York.

Panofsky, H. A., and G. W. Brier, 1958: Some Applications of Statistics to Meteorology, University Park, Pennsylvania.

Zuev, V. V., M. I. Andreev, V. D. Burlakov, A. V. El'nikov, and A. N. Nevzorov, 1998: Results of lidar studies of the structure and dynamics of cirrus clouds above western Siberia. In *Proceedings of the Eighth Atmospheric Radiation Measurement (ARM) Science Team Meeting*, DOE/ER-0738, pp. 871-879. U.S. Department of Energy, Washington, D.C.